DOI 10.1007/s10946-014-9435-2
Journal of Russian Laser Research, Volume 35, Number 4, July, 2014

A DIODE-PUMPED ACTIVELY *Q*-SWITCHED AND INJECTION-SEEDED Tm:LuAG LASER AT ROOM TEMPERATURE

Chunting Wu,[1,3]* Fei Chen,[2] and Youlun Ju[3]

[1]*School of Science*
Changchun University of Science and Technology
Changchun 130022, China

[2]*State Key Laboratory of Laser Interaction with Matter*
Changchun Institute of Optics, Fine Mechanics and Physics
Chinese Academy of Sciences
Changchun 130033, China

[3]*National Key Laboratory of Science and Technology on Tunable Laser*
Harbin Institute of Technology
Harbin 150080, China

*Corresponding author e-mail: bigsnow1 @ 126.com

Abstract

We elaborate a diode-end-pumped actively *Q*-switched injection-seeded Tm:LuAG laser. To achieve power scaling with good beam quality, we construct a more flexible laser with longer cavity accommodated strongly aberrated thermal lens in a Tm:LuAG laser and took special care in designing the laser resonator. Under *Q*-switched operation, we achieve a maximum output energy of 2.6 mJ with a pulse width of 318.2 ns at a pulse repetition frequency of 50 Hz. To control the spectral, temporal, and phase characteristics of the Tm:LuAG laser, the ring laser is injected by a seed laser, which provides a 50 mW single longitudinal-mode laser output at a wavelength of 2,022.6 nm. We achieve an output energy of 1.8 mJ with a pulse width of 293.0 ns after employing the injection seed.

Keywords: diode-pumped lasers, Tm laser, injection seed.

1. Introduction

All-solid-state lasers operating in the eye-safe spectral region near 2 μm are employed for medical applications, pumping mid-infrared optical materials using the parametric oscillations, and especially as sources for coherent laser-radar applications. The high power and long laser pulses of Tm,Ho co-doped and Tm-doped lasers enable them to be employed as light-beam sources of lidar systems due to their long upper laser-level lifetimes and small laser-transition effective cross-sections [1–4].

These laser systems have broad absorption lines centered at 785 nm, where efficient pumping diodes are available. Compared with Tm,Ho co-doped lasers, Tm-doped lasers are favorable for operating at room temperature due to a strong up-conversion effect in Tm,Ho co-doped lasers. This effect reduces the

Manuscript submitted by the authors in English first on August 7, 2013 and in final form on February 26, 2014.

effective energy-storage time of the Ho transitions, which is reduced to a value less than the intrinsic upper-state lifetime, resulting in a reduction of the energy-storage capacity and loss of conversion efficiency. Furthermore, it increases instabilities in the Q-switched operation regime [5, 6].

Tm:YAGs have been extensively studied since they have the advantages of high mechanical strength, high heat conductivity, and good thermal shock parameter; also they can provide high-power operation without fractures [7]. However, the diode-pumped thulium-doped $Lu_3Al_5O_{12}$ (Tm:LuAG) laser would be a more attractive source for atmospheric lidars due to two main reasons. On the one hand, an atmospheric lidar requires a laser source at a wavelength with a high atmospheric transmission. The maximum gain of the Tm:YAG laser is at a wavelength of 2,013 nm, which has a poor atmospheric transmission (-1.3 dB·km^{-1}). Usually, the output wavelength must be shifted to 2,020 nm if a Tm:YAG laser is used. The Tm:LuAG emission wavelength is centered at 2,023 nm, which is closer to the atmospheric transmission window. On the other hand, it is a quasi-three-level laser system for the Tm-doped laser operation, and the thermal population of the terminal laser level leads to significant ground-state reabsorption losses [8]. For a Tm:LuAG laser, the upper laser level is higher than that of a Tm:YAG laser, and the relatively lower-level population density makes the first one a more attractive laser medium for scaling the output power of 2 μm lasers at room temperature.

In the past few years, some characteristics of Tm:LuAG lasers have been investigated. In 1995, a total optical-to-optical efficiency of 7.3% and an optical-to-optical differential efficiency of 23.6% were achieved by diode-pumped Tm:LuAG lasers [9]. In 2000, a maximum output of 0.92 W was obtained from a diode-pumped Tm:LuAG laser at a pump power of 10 W [10]. In 2004, a 1 W laser diode in an end-pumped with four-pass geometry was used to achieve a Tm:LuAG laser output of 205 mW. Then a 51 mW single-frequency Tm:LuAG laser was obtained by inserting a 125 μm etalon into the laser resonator, where the Tm:LuAG (Tm^{3+}:10 at.%) crystal was 435 μm in length [11]. In 2008, a maximum output power of 4.91 W at 20 W diode-pump power was demonstrated, which corresponds to a slope efficiency of 25.39% [12]. Then, a 148 mW single longitudinal-mode Tm:LuAG laser was realized by combined use of a 0.1 mm silica etalon and a 1 mm YAG etalon [13]. However, the resonator mentioned above was either too simple or too short, and it was impossible to insert other components, like a Q-switch device. Also, because of the strongly aberrated thermal lens in the laser crystal, there was little work focused on characteristics of Q-switched Tm:LuAG lasers. Therefore, there exists an urgent need to develop a more flexible laser with a longer resonator to facilitate power scaling with good beam quality and, at the same time, accommodate a strongly aberrated thermal lens in the Tm:LuAG laser.

In this paper, we design a proper resonator for a Q-switched Tm:LuAG laser. We investigate the laser characteristics under the Q-switched operation at a pulse repetition frequency of 50 Hz. A pulsed laser diode is used to pump the Q-switched Tm:LuAG laser. The pulsed-pumping structure can reduce the thermal effect in the Tm:LuAG crystal and improve the output energy. We achieve a maximum output energy of 2.6 mJ with a pulse width of 318.2 ns at 50 Hz. Then we inject into the resonator a narrow-band radiation from a seed laser to control the spectral, temporal, and phase characteristics of the Q-switched Tm:LuAG laser. We achieve an output energy of 1.8 mJ with a pulse width of 293.0 ns after injection seeding. The build-up time of the laser pulse is reduced substantially. The beam quality, the stability of the Q-switched pulse, and the output energy are also improved after injection seeding.

2. Theoretical Analysis

For Tm^{3+}-doped quasi-three-level 2 μm lasers, there exist three main problems that restrict their power scaling. First, the saturation intensity for a laser transition is inversely proportional to the product of the emission cross-section and lifetime and the laser threshold. Therefore, low gain transitions lead to high saturation intensities. Second, compared with a four-level laser, a quasi-three-level transition requires more pump power to reach the threshold due to laser-photon reabsorption by the lower laser level. Third, nonradiative transitions and relaxation between the levels usually cause heating of the crystal host. These facts result in a series of effects, such as thermal lensing, end-face bulging, and so on.

In spite of the fact that the small emission cross-section is responsible for the increase in the pulse width, low gain transitions lead to high saturation intensities, which means a threshold increase. Then high intensity of the pump source is needed to decrease the threshold, which leads to thermal effects in the laser crystal. To limit the thermal effect, one needs a large-volume oscillating beam to maintain the power scale of the 2 μm laser output, especially in the Q-switched operation regime, because the thermal-lens focal lengths are short, the aberration increases the laser losses, and mode matching between the laser beam and the pump beam in the laser crystal becomes difficult. Taking into account the contradictions in the process of solving the problems mentioned above, an appropriate resonator design becomes of particular importance.

In this paper, we design a ring laser to eliminate the problem of limits in the laser efficiency and the deterioration of the spectral characteristics in linear resonators due to the presence of spatial hole burning of the laser. Also the bidirectional output of the ring laser is appropriate to use it as a slave laser (power laser) for an injection-seeded laser (master laser), since injection can be easily made from one direction. Then the nonselective slave laser can provide a powerful and, at the same time, highly selective laser output along with controlling its spectral, temporal, and phase characteristics by seeding a narrow-band radiation from the master laser. Also, in the same capacity, the ring laser has a longer cavity to ensure a large-volume oscillating beam and a long pulse-width output. Nevertheless, to decrease the threshold of a quasi-three-level laser operating at the low-gain transition, the cavity length should not be too long. The laser oscillator is a bow-tie cavity with a length of 0.3 m, as shown in Fig. 1. The strategy employed here is to use the laser-resonator response for producing changes in the mirror curvature and arm lengths in order to partially offset the aberrations and increase the strength of the thermal lens.

Two plane mirrors M1 and M2 are set on facets of the laser crystal. Two concave mirrors M3 and M4 with the same radius of curvature $\sim$5 m are positioned on facets of the Q-switch crystal. The thermal lens of the crystal is seen as a parabolic thin lens, which is convenient for the resonator design using the ABCD matrices. While considering the thermal focal lens in the gain medium (the laser-beam radius at two facets of the laser crystal), we calculate the two facets of the Q-switch crystal using Matlab software, as shown in Fig. 2. The stability of the cavity versus the thermal lens is expressed as $(A + D)/2$ and shown in Fig. 2. We see that the laser cavity is not sensitive to the thermal lens and can stably operate at high-pump levels. As long as the thermal lens is longer than 80 mm, $\dfrac{d\omega}{df} \approx 0$. The beam radii at two facets of the laser crystal are about 0.41 mm, which helps one to relieve thermal effects. The pump beam in the laser crystal is 0.8 mm in diameter for good mode matching with the laser beam. The beam radius at two facets of the Q-switch crystal is $\sim$0.31 mm, which is quite proper not only to protect the coating film from fraction but also to keep shorter the transit time of Q switching.

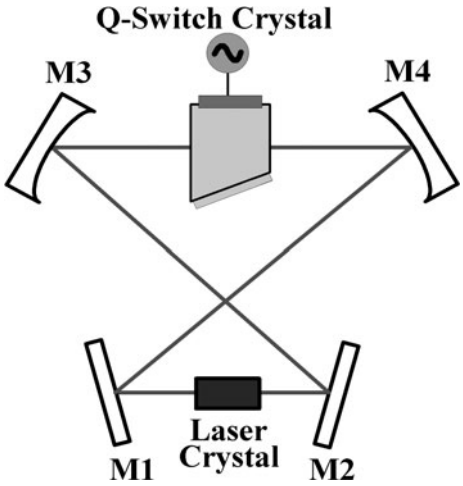

Fig. 1. Schematic of a bow-tie cavity.

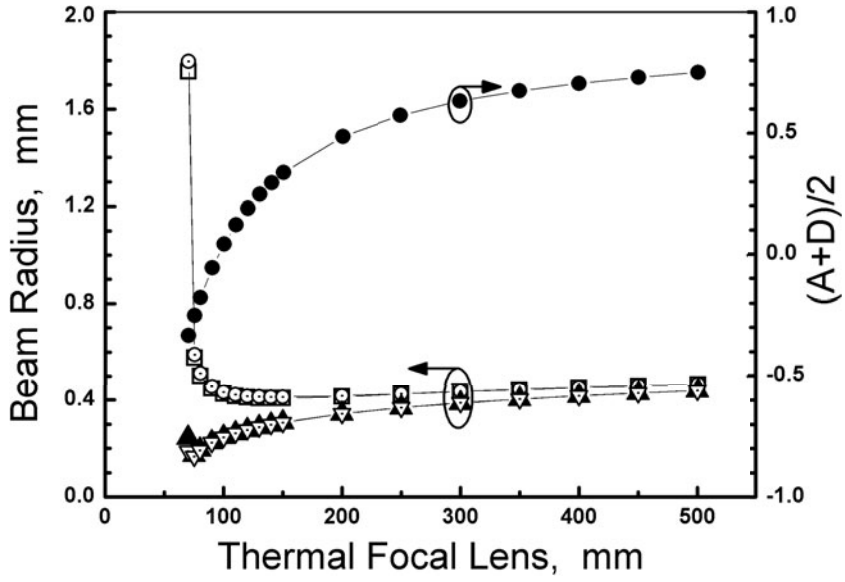

Fig. 2. Laser-beam radii in the laser and Q-switch crystals (left y axis) and the stability of the cavity (right y axis) versus the thermal focal length for optical-fiber output 1 (□) and optical-fiber output 2 (○) of the Tm:LuAG crystal and for optical-fiber output 1 (▲) and optical-fiber output 2 (▽) of the Q-switch crystal.

3. Experimental Setup

Figure 3 shows the experimental setup of a Tm:LuAG laser system. The fiber-coupled laser diode (LD) is employed as a pump source, which delivers a maximum peak power of 30 W at 788 nm from the output of an optical fiber with 400 μm core diameter and N.A. = 0.22. The pump beam is coupled to the gain medium by coupling optics, and the light-beam-spot radius generated in the crystal is equal to 800 μm in order to be matched with the laser beam. The total transmission efficiency of the beam-reshaping system is ∼92% at 788 nm. A major advantage of 2 μm Tm lasers for efficient operation is the cross-relaxation process that could provide two ions in the upper laser level for one pump photon ($^3H_4$+$^3H_6$–$^3F_4$+$^3F_4$). However, the two-for-one pumping efficiency requires high doping levels, and lower Tm^{3+} concentrations can be beneficial in distributing the thermal load for the end pumping and reducing the ground-state reabsorption losses at the laser wavelength. We choose a Tm:LuAG crystal with a Tm^{3+}-doping concentration of 4 at.% and dimensions of 3×3×7 mm^3 as the gain medium, which has been proved to have better laser characteristics than a Tm^{3+}-doping concentration of 6 at.% in our previous experiments. The crystal was wrapped with 0.1 mm thick indium foil and held in a brass heat sink. The temperature of the heat sink was kept constant, 290±0.07 K, with

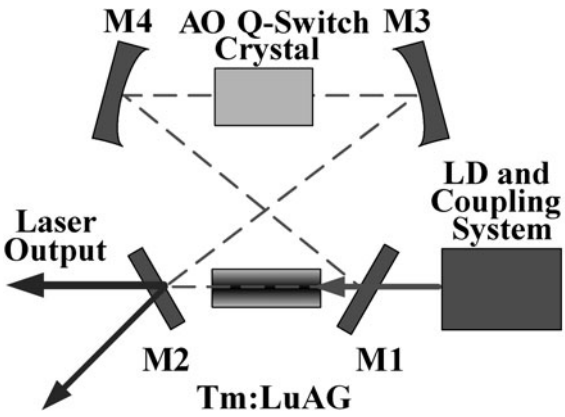

Fig. 3. Experimental setup of a Tm:LuAG laser system.

the help of a thermoelectric cooler.

The experiments were carried out with a bow-tie cavity, which consisted of a flat dichroic input mirror M1, a flat output coupler M2, and two concave mirrors M3 and M4. Both radii of curvature for M3 and M4 are 5 m. The total cavity length is 0.3 m. A 46 mm long fused-silica acousto-optical Q-switch was inserted into the resonator to provide a Q-switched operation regime. Both output facets of the modulator were antireflection coated at 2020 nm (R<0.5%). The maximum power was 50 W, and intrinsic diffraction losses were 85%, which was reasonable to prevent lasing operation. As mentioned above, the laser cavity was designed carefully to allow mode matching between the laser beam and the pump beam in the Tm:LuAG crystal and to provide the proper spot size in the Q-switch crystal. The minimum folded angle was set to ∼21.3°.

4. Experimental Results and Discussion

In our experiments, we used the knife-edge method to measure the intensity profile of the laser beam under Q-switched operation at 50 Hz through a waist formed by a lens ($f = 150$ mm). Then we calculated the laser-beam radius and the full-angle divergence versus the position of the output coupler. The thermal-lens influence should be taken into account in the ABCD matrix. We verified the focus of the thermal lens (up to coincidence with the radius of the laser beam) until the full-angle divergence on the output-coupler position coincided with the experimental result. The thermal lens estimated by this method is 150 mm, and the beam radius is about 0.41 mm at both facets of the laser crystal and 0.31 mm at both facets of the Q-switch crystal for a thermal focal lens of 150 mm. The parameter $(A + D)/2$ is 0.0085. The beam radius in the cavity with a thermal focal lens of 150 mm is shown in Fig. 4. In the whole device, the sagittal and tangential beams are in strong concurrence (in contrast to the ideal beam), which means that the astigmatism losses are small. Under these conditions, we achieved a stable Q-switched operation regime. In spite of the fact that the mode matching between the laser and pump beams was good enough, the pump-beam spot radius in the crystal should be increased up to ∼1.2 mm in order to reduce the intensity of the pump power and decrease the thermal effect.

We employed output couplers with transmissions of 2.0, 2.97, 3.5, and 5.0%; our best calculated results were obtained for 2% at the free-running oscillations, and for 3.5% at the Q-switched operation regime. Our best experimental results were obtained when we employed an output coupler with a transmission of 3.5%.

The pulse width versus the output energy of the Q-switched Tm:LuAG laser operating at a pulse repetition frequency of 50 Hz is shown in Fig. 5. We used an energy meter to measure the output energy and study the output-pulse width employing a TDS3032B digital oscilloscope (Tektronix Inc., USA) and a room-temperature mercury-cadmium-telluride photoconductive detector with a response time of 1 ns. We observed a decrease in the pulse width with increase in the output energy. An output energy equal to 2.6 mJ with a pulse width of 318.2 ns and a slope efficiency of 6.7% were obtained at a repetition frequency of 50 Hz, which is better than in our previous work [14]. The beam quality of the output laser $M2$ was 1.3 (measured by the traveling 90/10 knife-edge method at the maximum output energy). We measured the output wavelength using a monochrometer (300 mm focal length, 300 lines/mm grating blazed at 2000 nm) and detected the input laser using an InGaAs detector connected with a digital oscilloscope (Tektronix TDS3032B). The peak output wavelength was 2,022.79 nm, which serves as a guide for the injection locking.

It is a common knowledge that diode lasers used in LIDAR systems should have long-pulse-width

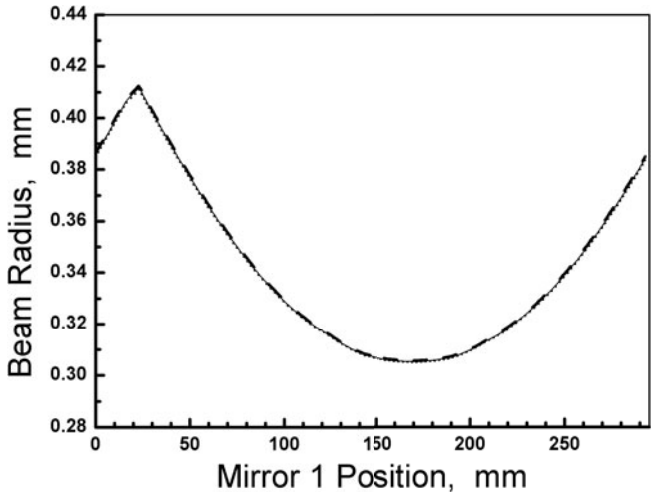

Fig. 4. The beam radius in the ring cavity with the thermal focus lens ($f = 150$ mm). Here, sagittal (dotted curve), tangential (dashed curve), and ideal (solid curve) beams.

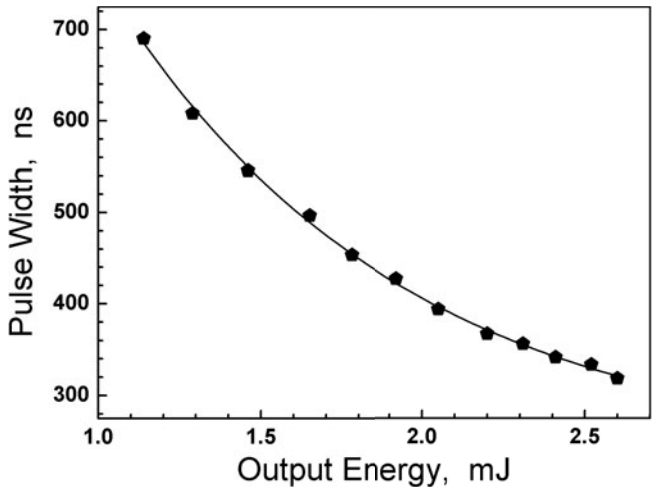

Fig. 5. Pulse width versus the output energy of the Q-switched Tm:LuAG laser operating at a pulse repetition frequency of 50 Hz.

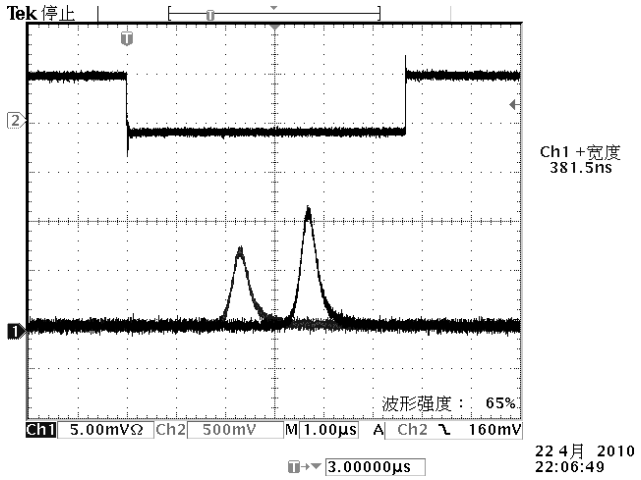

Fig. 6. Temporal pulse shapes of the injection-seeded Q-switched pulse and the usual Tm^{3+}-doped diode-laser pulse.

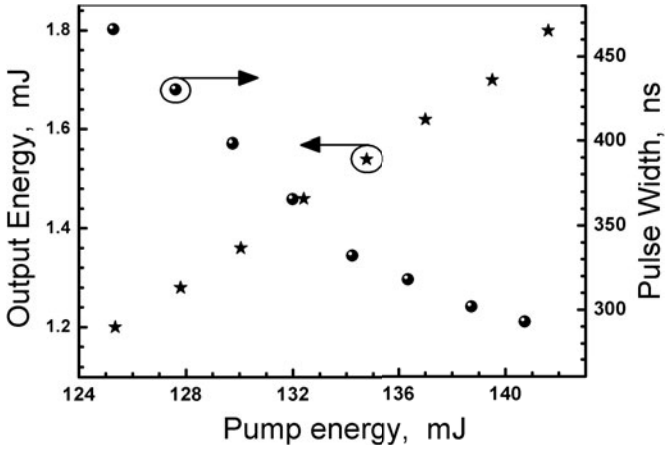

Fig. 7. Output energy and pulse width of the injection-seeded laser versus incident pump energy.

laser outputs, and this is the reason why we investigate the characteristics of injection-seeded Tm:LuAG lasers at 50 Hz. To control the spectral, temporal, and phase characteristics, the ring laser was injected by a narrow-band radiation from a seed laser, which provided a 50 mW single-longitudinal-mode laser output with a wavelength of 2,022.6 nm. First, we provided effective coupling between the two lasers; then an InGaAs detector was placed behind mirror M3 to detect the seed resonance signal penetrating through the mirror. While the optical signal is transformed into an electric signal and then transmitted to the controlling system, two commands are executed to the pump source and to the Q switch. Thus, the power oscillation frequency matches the frequency of the seed laser, which improves the spectral purity of the output. Note that the Q-switched laser-output energy should be relatively constant versus

the Q-switch-delay trigger time to minimize energy fluctuation.

The pulse-jumping phenomenon from the frequency-unlocked regime to the frequency-locked regime is shown in Fig. 6. We see that the build-up time of the laser pulse is obviously reduced after injection seeding. Also injection locking improves the stability of the Q-switched pulse and the output energy. A pulse width equal to 293 ns is achieved at an injection seeded energy equal to 1.80 mJ. The output energy and pulse width of the injection-seeded laser versus the incident pump energy is shown in Fig. 7.

The build-up time of the laser output pulse is defined by the competition between the injection-driven field and the noise-driven field. The locking regime takes place when the intensity ratio of the two competing fields exceeds a given signal-to-noise ratio at the saturation time. Figure 8 shows the build-up time of the injection-seeded laser versus the output energy (for comparison, we also show the same characteristic for the usual Tm^{3+}-doped diode laser). We see that the build-up time is reduced for the injection-seeded laser. In addition, we see in Fig. 9 that the injection-seeded laser radiates in only one direction, the stability is improved substantially, and $M2 = 1.14$ (measured by the same 90/10 knife-edge method).

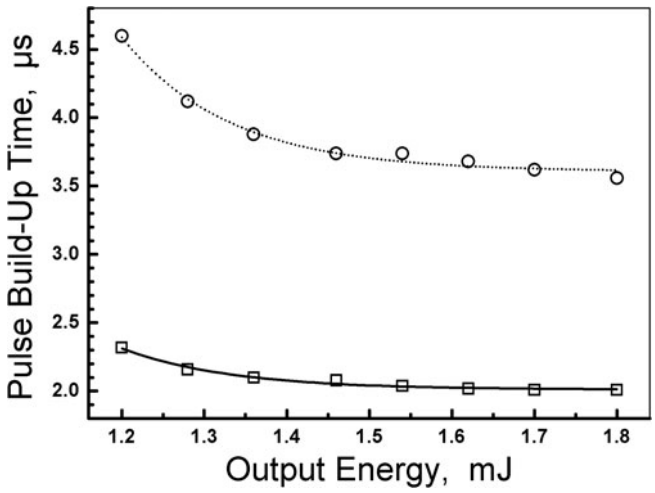

Fig. 8. Pulse build-up time of the injection-seeded laser versus output energy without frequency locking (○) and with frequency locking (□).

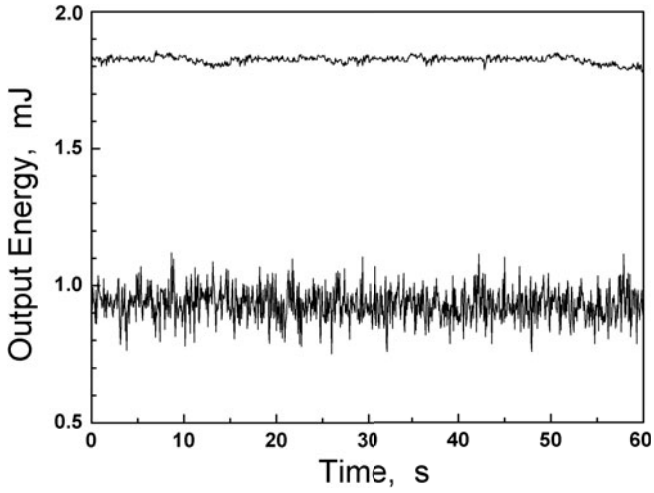

Fig. 9. Output-energy stability of the injection-seeded laser (upper curve) and the same for the usual Tm^{3+}-doped laser (lower curve).

5. Summary

To conclude, we elaborated a diode-pumped Q-switched quasi-three-level Tm:LuAG laser. To achieve power scaling with good beam quality, we developed a more flexible laser with a longer cavity and accommodated a strongly aberrated thermal lens in a Tm:LuAG laser; also we took special care to design the resonator. In the Q-switched operation regime, we investigated the laser characteristics such as the output energy, pulse width, output wavelength, and beam quality at a pulse repetition frequency of 50 Hz. To control the spectral, temporal, and phase characteristics of the Tm:LuAG laser, we injected the ring laser by a seed laser and reached an output energy equal to 1.8 mJ with a pulse width of 293.0 ns. We showed that the beam quality, Q-switched pulse stability, and output energy were improved in the laser we elaborated.

References

1. G. J. Koch, J. P. Deyst, and M. E. Storm, *Opt. Lett.*, **18**, 1235 (1993).
2. H. Jelínková, P. Koranda, M. E. Doroshenko, et al., *Laser Phys. Lett.*, **4**, 23 (2007).
3. C. T. Wu, F. Chen, R. Wang, and Y. L. Ju, *J. Russ. Laser Res.*, **33**, 98 (2012).
4. C. T. Wu, F. Chen, and Y. L. Ju, *J. Russ. Laser Res.*, **34**, 103 (2013).
5. T. S. Kubo and T. J. Kane, *IEEE J. Quantum Electron.*, **28**, 1033 (1992).
6. C. Li, J. Song, N. S. Kim, and K. Ueda, *Opt. Exp.*, **4**, 12 (1999).
7. O. A. Buryy, D. Y. Sugak, S. B. Ubizskii, et al., *Appl. Phys. B*, **88**, 433 (2007).
8. J. D. Kmetec, T. S. Kubo, and T. J. Kane, *Opt. Lett.*, **19**, 186 (1994).
9. N. P. Barnes, M. G. Jani, and R. L. Hutcheson, *Appl. Opt.*, **34**, 4290 (1995).
10. V. Wulfmeyer, M. Randall, A. Brewer, and R. M. Hardesty *Opt. Lett.*, **25**, 1228 (2000).
11. K. Scholle, E. Heumann, and G. Huber, *Laser Phys. Lett.*, **1**, 285 (2004).
12. C. T. Wu, Y. L. Ju, Y. F. Li, et al., *Chin. Opt. Lett.*, **6**, 415 (2008).
13. C. T. Wu, Y. L. Ju, Z. G. Wang, et al., *Laser Phys. Lett.*, **5**, 510 (2008).
14. F. Chen, C. T. Wu, Y. L. Ju, et al., *Laser Phys.*, **22**, 371 (2012).